Membrane Electrical Activity Elicits Inositol 1,4,5-Trisphosphate-dependent Slow Ca^{2+} Signals through a $G\beta\gamma$/Phosphatidylinositol 3-Kinase γ Pathway in Skeletal Myotubes*

José M. Eltit[‡1], Alejandra A. García[‡], Jorge Hidalgo[‡], José L. Liberona[‡], Mario Chiong[§], Sergio Lavandero[‡§], Edio Maldonado[‡], and Enrique Jaimovich[‡2]

From the Centro de Estudios Moleculares de la Célula, Instituto de Ciencias Biomédicas, Facultades de [‡]Medicina y [§]Ciencias Químicas y Farmacéuticas, Universidad de Chile, Independecia 1027, Santiago 7, Chile

Tetanic electrical stimulation of myotubes evokes a ryanodine receptor-related fast calcium signal, during the stimulation, followed by a phospholipase C/inositol 1,4,5-trisphosphate-dependent slow calcium signal few seconds after stimulus end. L-type calcium channels (Cav 1.1, dihydropyridine receptors) acting as voltage sensors activate an unknown signaling pathway involved in phospholipase C activation. We demonstrated that both G protein and phosphatidylinositol 3-kinase were activated by electrical stimulation, and both the inositol 1,4,5-trisphosphate rise and slow calcium signal induced by electrical stimulation were blocked by pertussis toxin, by a $G\beta\gamma$ scavenger peptide, and by phosphatidylinositol 3-kinase inhibitors. Immunofluorescence using anti-phosphatidylinositol 3-kinase γ antibodies showed a clear location in striations within the cytoplasm, consistent with a position near the I band region of the sarcomere. The time course of phosphatidylinositol 3-kinase activation, monitored in single living cells using a pleckstrin homology domain fused to green fluorescent protein, was compatible with sequential phospholipase Cγ1 activation as confirmed by phosphorylation assays for the enzyme. Co-transfection of a dominant negative form of phosphatidylinositol 3-kinase γ inhibited the phosphatidylinositol 3-kinase activity as well as the slow calcium signal. We conclude that $G\beta\gamma$/phosphatidylinositol 3-kinase γ signaling pathway is involved in phospholipase C activation and the generation of the slow calcium signal induced by tetanic stimulation. We postulate that membrane potential fluctuations in skeletal muscle cells can activate a pertussis toxin-sensitive G protein, phosphatidylinositol 3-kinase, phospholipase C pathway toward modulation of long term, activity-dependent plastic changes.

The role of the voltage-dependent calcium channel (Cav 1.1) or dihydropyridine receptor (DHPR)[3] in excitation-contraction (EC) coupling in skeletal muscle is well known (1–4). Recently, another sequence of molecular processes activated by cell membrane depolarization involving the DHPR also acting as membrane voltage sensor has been reported.

A slow calcium signal, first described in rat myotubes stimulated with K^+ depolarization, occurs several seconds after the fast calcium signal that is due to ryanodine receptor opening and mediates EC coupling. The former is refractory to ryanodine treatment and depends on inositol 1,4,5-trisphosphate (IP_3) generation (5, 6). This slow calcium signal has a predominant nuclear component, and its propagation between adjacent nuclei in the myotube can be frequently recorded (5). Besides the fact that the three types of IP_3 receptors are located at different sites within rat myotubes, including the nuclear region, a functional calcium store in isolated nuclei has been recently described (7). Treatment of these isolated nuclei with IP_3 induces calcium release to the nucleoplasm, regulating phosphorylation of the transcription factor cAMP response element-binding protein (7). The slow calcium signal appears to participate in the regulation of transcription factors and the modulation of gene expression mediated by membrane depolarization and calcium via an IP_3 signaling pathway (8–10). In addition, a slow calcium signal localized near the motor endplate of depolarized adult muscle fibers was associated to a region rich in IP_3 receptor (11).

The molecular mechanism involved in phospholipase C (PLC) activation induced by membrane depolarization is still not understood but in several systems, G protein-dependent PLC activation has been described. Both $G\alpha_q$ and $G\beta\gamma$ (released from heterotrimeric $G_{i/o}$) may directly activate PLCβ isoforms. Also, $G\beta\gamma$ may indirectly activate PLCγ increasing phosphatidylinositol 3,4,5-trisphosphate (PIP_3) levels by activation of phosphatidylinositol 3-kinase (PI3K) γ (12, 13).

When, tetanic electrical field stimulation was used instead of K^+ depolarization, an enhanced IP_3-dependent, slow calcium signal was observed, and again the DHPR was necessary to sense the action potentials induced by the stimulation protocol (14). In this work we test the hypothesis that tetanic electrical stimulation of myotubes activates both G protein and PI3K and that both signaling pathways are required for the activation of PLC and the onset of the slow calcium signal. We now present evidence that both $G\beta\gamma$ and PI3Kγ are activated by tetanic stimulation and are involved in the generation of the slow calcium signal. Moreover, we found that electrical stimulation induce PLCγ1 phosphorylation in both cytoplasm and nuclear envelope suggesting that the $G\beta\gamma$/PI3Kγ pathway could be involved in the transduction of the electrical message in the T-tubule membrane to an IP_3-dependent calcium signal in the nucleus. This is the first study to suggest a role for the

* This work was supported in part by the Fondo Nacional de Investigación en Areas Prioritarias (Grant 15010006 to E. J. and S. L.) and by National Institutes of Health Fogarty International Research Collaboration Award RO3TW07053-01. The costs of publication of this article were defrayed in part by the payment of page charges. This article must therefore be hereby marked "*advertisement*" in accordance with 18 U.S.C. Section 1734 solely to indicate this fact.

[1] Holds a Ph.D. fellowship from the Comisión Nacional de Investigación Científica y Tecnológica.

[2] To whom correspondence should be addressed. Tel.: 562-978-6067; Fax: 562-735-3510; E-mail: ejaimovi@med.uchile.cl.

[3] The abbreviations used are: DHPR, dihydropyridine receptor; EC, excitation-contraction; IP_3, inositol 1,4,5-trisphosphate; PLC, phospholipase C; PTX, pertussis toxin; PIP, phosphatidylinositol monophosphate; PIP_2, phosphatidylinositol 4,5-bisphosphate; PIP_3, phosphatidylinositol 3,4,5-trisphosphate; PI3K, phosphatidylinositol 3-kinase; PH, pleckstrin homology; BTK, Bruton's tyrosine kinase; GFP, green fluorescent protein; GST, glutathione *S*-tranferase; ctβARK, carboxyl terminus of the β-adrenergic receptor kinase; Ad, adenoviral vectors; LY, LY294002; wt, wild type; EV, empty viral construct; KR, kinase-inactive; DsRed, red fluorescent protein.

Gβγ/PI3Kγ pathway in the development of a depolarization-dependent calcium signal in excitable cells.

EXPERIMENTAL PROCEDURES

Primary and 1B5 Cell Cultures—Rat myotubes primary cultures were prepared as detailed previously (5, 14). The dyspedic skeletal muscle cell line (1B5) was kindly provided by Dr. Paul D. Allen (Brigham and Women's Hospital, Boston, MA). These cells were transiently transfected using FuGENE 6 (Roche Applied Science) following the manufacturer's instructions. The plasmids used encode the fusion protein between the pleckstrin homology (PH) domain of Bruton's tyrosine kinase (BTK) and the enhanced green fluorescent protein (GFP) ((PH)BTK-GFP) or the (PHmut)BTK-GFP (punctual mutation R28C of the PH domain). Both plasmids were kindly provided by Dr. Tamas Balla (National Institutes of Health, Bethesda, MD) (15). A plasmid encoding enhanced GFP was also used. Alternatively, (PH)BTK-GFP was co-transfected with a plasmid encoding the kinase-inactive p110γ K799R (PI3Kγ(KR)) (16, 17), the wild-type enzyme (wt), the membrane-targeted CAAX-PI3Kγ wt, or the membrane-targeted inactive kinase CAAX-PI3Kγ (KR). These p110γ plasmids and a monoclonal anti-p110γ antibody were kindly provided by Dr. Matthias P. Wymann (University of Fribourg, Switzerland). Also, these PI3Kγ plasmids were co-transfected with monomeric DsRed (Clontech, Palo Alto, CA) as transfection marker, and the calcium signals of the transfected cells were measured using Fluo3 (see below).

Incubation of Cells and Calcium Measurements—Cells were incubated with 40 μM LY294002 (LY, Calbiochem), 100 nM wortmannin (Sigma-Aldrich), or for at least 4 h with 1 μg/ml PTX (Calbiochem). Adenoviral transfection is described below. For calcium measurements, cells were loaded with 5.5 μM Fluo3-AM (Molecular Probes, Eugene, OR) in Krebs buffer (145 mM NaCl, 5 mM KCl, 1 mM $CaCl_2$, 1 mM $MgCl_2$, 5.6 mM glucose, 10 mM HEPES-Na, pH 7.4) in the presence of the pharmacological agent to be tested for 40 min, washed three times and incubated in Krebs solution, also in the presence of the drug. Alternatively for the calcium-free condition, the washout and the measurement were performed in calcium-free saline (145 mM NaCl, 5 mM KCl, 2 mM $MgCl_2$, 0.5 mM EGTA, 5.6 mM glucose, 10 mM HEPES-Na, pH 7.4). As control, the vehicle instead of the drug was used. The electrical field stimulation (400 pulses of 1 ms at 45 Hz were used in all experiments except when indicated), and calcium signal acquisition was performed as was previously described (14).

Action Potential Measurements—Membrane potential was measured with ~40 MΩ tip resistance microelectrodes, filled with 1 M potassium glutamate, 20 mM KCl, pH 7.4. An Ag/AgCl electrode in a salt bridge filled with the same solution was used as ground reference. The microelectrode was connected to a Micro-Probe System Model M-707 (WPI, Sarasota, FL). The output was offset-corrected, and capacity was compensated and then digitized by an analog to digital converter (Labmaster DMA, Scientific Solutions, Mentor, OH). Trains of 20 pulses of 1 ms delivered at 2, 10, or 45 Hz were used; spontaneous action potentials were also observed.

Enhanced GFP and Fluo3 AM Fluorescence Acquisition by Confocal Microscopy—Transfected 1B5 cells or primary myotubes loaded with Fluo3-AM were placed in an inverted microscope (Carl Zeiss, Axiovert 200) coupled to an LSM 5-pascal confocal attachment. An argon laser at 488 nm was used as the excitation source, the laser power was used in the standby position at 1% of transmission to avoid photobleaching, and the emission was collected in one channel equipped with a 505–530 nm bandpass filter. The electrical stimulation was delivered by an independent device (14). Image processing was performed off-line with ImageJ software.[4] Graphs were generated using Origin 6.0 (OriginLab, Northampton, MA).

IP_3 Measurements—Cells were exposed to pharmacological agents as described above or were transfected with adenovirus. An electrical field stimulator device previously described (14) was used. The method used for IP_3 measurement was detailed previously (5, 14).

Gβγ Pull-down Assay—The fusion protein between glutathione *S*-transferase and the carboxyl terminus of the β adrenergic receptor kinase (GST-ctβARK) or the GST alone was expressed and purified as described previously (19). The plasmid encoding the fusion protein was kindly provided by Dr. Robert J. Lefkowitz (Duke University Medical Center). After stimulation, 100 μl of ice-cold lysis buffer (0.1% Triton X-100, 0.1% sodium deoxycholate, 125 mM NaCl, 20 mM Tris-HCl, pH 7.5) containing protease inhibitor mixture set III (Calbiochem) was added and centrifuged (10 min at 20,000 × *g*). Ten microliters of the supernatant was separated for the total Gβ determination (SDS-PAGE, see below). To the remaining extract, 200 μl of binding buffer (50 mM Tris HCl, 10 mM $MgCl_2$, 0.5 mg/ml bovine serum albumin, 0.5 mM dithiothreitol, 100 mM NaCl, pH 7.5) and 60 μg of the recombinant protein immobilized in the glutathione-agarose resin were added. After 45-min incubation at 4 °C with rotation, the agarose beads were washed three times with cold binding buffer, and retained proteins were removed from the beads with SDS-PAGE sample buffer, subjected to SDS-PAGE on 15% acrylamide gels, and transferred to a polyvinylidene difluoride membrane. Monoclonal antibodies against β subunit G protein (BD Biosciences, San Jose, CA) were used, and the blots were developed with an anti-mouse antibody conjugated to alkaline phosphatase (Pierce Biotechnology, Rockford, IL). Results were calculated as the relative amount of activated Gβ (pull down) corrected by the total amount of Gβ for each condition. Routinely, membranes were stained with Ponceau Red to check the equal amount of recombinant protein loaded (data not shown).

PIP_3 Measurements—Cultured myotubes were incubated in Krebs solution (phosphate-free) for 1 h. Then the cells were switched to Krebs plus 50 μCi/ml $^{32}PO_4$ for 1.5 h. After stimulation the cells were scraped in 1 ml of ice-cold 2.5 M HCl, and the lysates were transferred to borosilicate glass test tubes. The chloroform extraction of phospholipids and the TLC development condition were performed as described previously (20). Radioactive spots were detected by autoradiography. Spots from PIP, PIP_2, and PIP_3 were scraped and counted in a liquid scintillation counter (Beckman Instruments). The counts of PIP_3 were corrected by dividing PIP plus PIP_2 counts as internal controls, and the results were expressed as -fold over the control condition. At least 70% of the counts recovered from the TLC spot correspond to PIP_3, evaluated by deacylation and high-performance liquid chromatography (20).

Immunofluorescence—Cultured myotubes were processed as previously reported (8). The primary antibodies were a polyclonal (rabbit) anti-p110γ (Santa Cruz Biotechnology, Santa Cruz, CA), a monoclonal (mouse) anti-α-actinin (BD Biosciences, San Jose, CA), monoclonal (mouse) anti-fast myosin (Sigma-Aldrich), monoclonal (mouse) anti-α1S DHPR (ABR, Golden, CO), monoclonal (mouse) anti-PLCγ1 (BD Biosciences), a polyclonal (rabbit) anti-phospho-PLCγ1 (Santa Cruz Biotechnology), and a monoclonal (mouse) anti-LAP2 (BD Biosciences). As secondary antibodies an anti-rabbit IgG conjugated to Alexa 488 and an anti-mouse IgG conjugated to Alexa 633 (Molecular Probes, Eugene, OR) were used for co-localization of PI3Kγ with the indicated markers. And as secondary antibodies an anti-rabbit IgG conjugated to Alexa 633 and an anti-mouse IgG conjugated to Alexa 488

[4] W. S. Rasband (1997) rsb.info.nih.gov/ij.

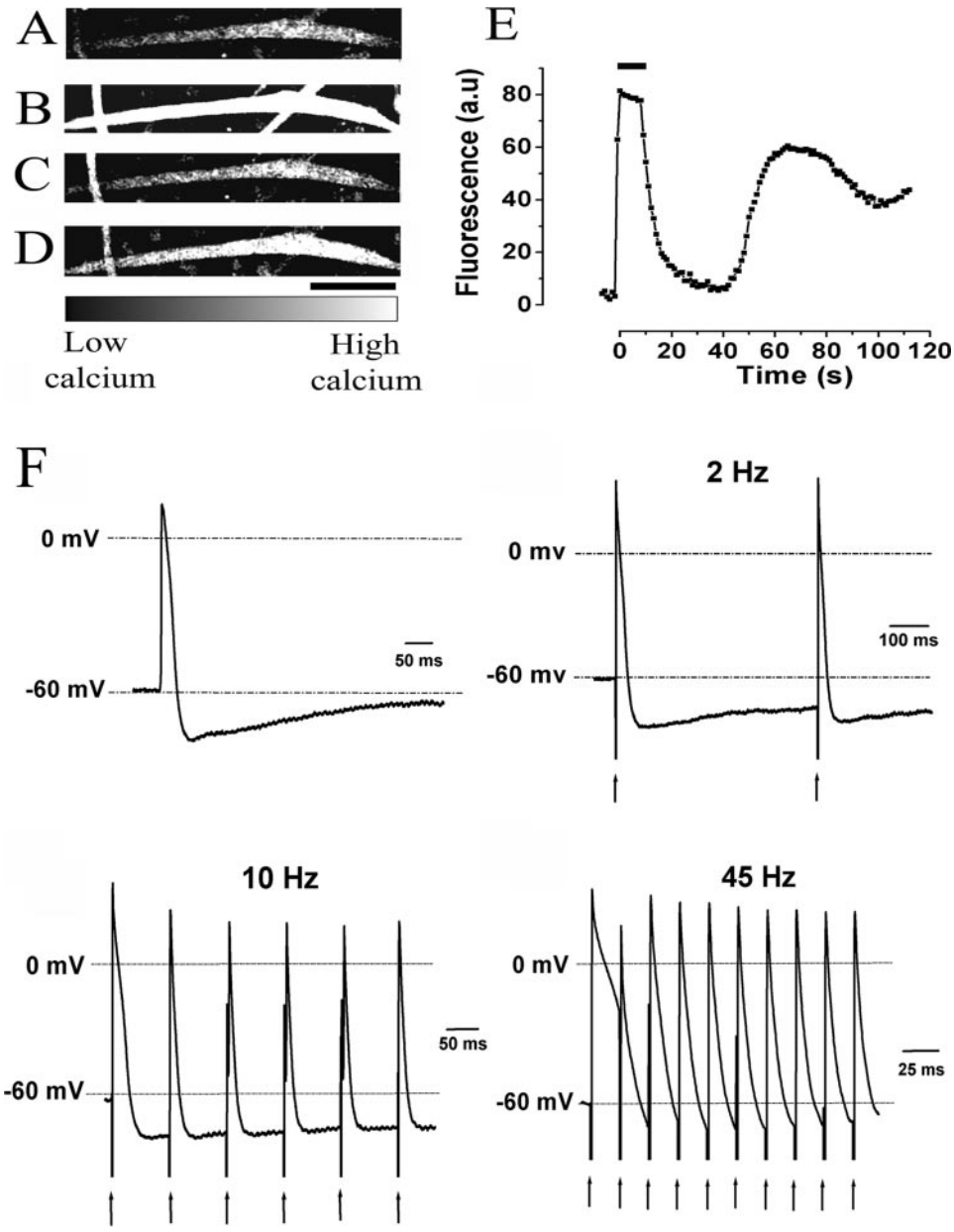

FIGURE 1. **Fast and slow calcium signal evoked by electrical stimulation.** Intracellular calcium levels were monitored in Fluo3-AM-loaded myotubes. The stimulation protocol was 400 pulses of 1-ms duration at 45 Hz (*black bar*). The images were acquired by confocal microscopy every 1 s. *A*, the basal fluorescence before the electrical protocol was applied. *B*, generalized increase of calcium in whole cells during the stimulation according with the EC-coupling mechanism. *C*, fluorescence image taken 13 s after the stimulation ended where the intracellular calcium returns to basal levels. *D*, increase of fluorescence corresponding to the slow calcium response that lasted for minutes. *Scale bar*, 50 μm. *E*, plot of the fluorescence during the whole experiment. Action potentials induced by field stimulation measured by an intracellular microelectrode. *F*, spontaneous action potential, induced by 1-ms pulse at 2 Hz, 10 Hz, and 45 Hz are shown. The *lower arrows* show the moment of stimulation. At 45 Hz it is shown that every stimulus elicits an action potential.

was used when co-localization of pPLCγ1 with the indicated marker was studied. The double-labeled preparations were observed in a confocal microscope (Carl Zeiss, Axiovert 200, LSM 5-pascal, argon laser at 488 nm for Alexa 488 and HeNe laser at 633 nm for Alexa 633). A single track acquisition was done, collecting emission in one channel the 505–530 bandpass signal for Alexa 488 and the 650 longpass signal in the other channel for Alexa 633. Images were deconvoluted using Iterative deconvolution software of Image J,[4] and the point spread function was calculated for each objective lens using calibrated fluorescent beads. Brightness and contrast were adjusted off-line to improve clarity for each image; no data were added or deleted. For phospho-PLC experiments, comparison between stimulated and non-stimulated condition was performed with identical acquisition settings.

Recombinant Adenoviruses—Adenoviral vectors (Ad) were propagated and purified as previously described (21). Two transgenes (a gift from Dr. W. J. Koch, Duke University Medical Center) were used: ctβARK (AdβARK) and an empty viral construct (EV). The ctβARK construct is a peptide inhibitor of G$\beta\gamma$ signaling (22). Myotubes were infected with adenoviral vectors at a multiplicity of infection of 1000 at least 48 h before were used for the indicated experiments.

Statistical Analysis—Data of n experiments were expressed as mean $\pm$ S.E. and were analyzed by one-way analysis of variance followed by Tukey's post test for comparison between groups. A p value < 0.05 was considered to be statistically significant.

RESULTS

Fast and Slow Calcium Signal Induced by Electrical Stimulation—To illustrate both the fast and slow calcium signals evoked by the same electrical stimulation, intracellular calcium was monitored by the Fluo3 fluorescence in loaded myotubes and visualized by confocal microscopy. Fluorescence image previous to stimulation (Fig. 1*A*) represents the basal level. During stimulation, a generalized calcium increase saturating the dye was induced (Fig. 1*B*). It is directly associated to the EC coupling mechanism, and cell contraction was visualized accordingly (data not shown). Seconds after, fluorescence returned to basal levels (Fig. 1*C*, 13 s after stimulation ended). 30–40 s after stimulation; the

slow calcium signal arose, whereas cell contraction was absent (data not shown). Fluorescence during the slow calcium signal, 65 s after stimulus ended can be appreciated (Fig. 1*D*). The time course of changes in calcium levels in a single cell (Fig. 1*E*), can be seen during an experiment in which each image was acquired every 1 s. The signals depicted here illustrate the response of a single cell; a detailed statistical study of the two types of signals induced by electrical stimulation was published (14).

In our previous work we demonstrated that field stimulation induces action potentials that in turn trigger both calcium signals (14). To define the relationship between extracellular stimulation and action potential induction at different stimulation frequencies, the membrane potential was monitored with an intracellular microelectrode. Fig. 1*F* shows action potentials elicited in the same cell by extracellular field stimulation using 1-ms pulses at 2, 10, and 45 Hz. The time needed to restore the resting membrane potential after the spike for a spontaneous action potential was 33.6 ± 1.1 ms; at 2 Hz external stimulation was 24.8 ± 0.2 ms, at 10 Hz was 19.6 ± 0.3 ms, and it was 15.1 ± 0.3 ms at 45 Hz. These results show that the myotube shortens the action potential duration by increasing the repolarization rate in response to higher stimulation frequencies, ensuring the generation of one action potential for each stimulation pulse at all the frequencies within the tested range.

A G Protein Is Activated by Electrical Stimulation—To identify the relationship between changes in membrane potential and G protein activity, we assessed G protein activation using a pull-down assay. When G protein is activated, the α subunit binds GTP and the $\beta\gamma$ dimer is released. Both GTP-α and $\beta\gamma$ subunits have downstream targets (23). A molecular tool, frequently employed to study the participation of the $\beta\gamma$ subunits in signaling pathways is the carboxyl terminus of the β adrenergic receptor kinase (ctβARK) that binds to the $\beta\gamma$ dimer, which, working as scavenger, blocks its actions (22). To measure G protein dissociation (upon activation), the ctβARK peptide fused to glutathione *S*-transferase (GST) was expressed and purified as described under "Experimental Procedures," together with GST alone as a control (Fig. 2*A*). The recombinant protein immobilized in a glutathione-agarose resin was used as bait for affinity purification of $\beta\gamma$ subunits in a pull-down assay, using lysates of myotubes previously subjected to electrical stimulation protocols. As control, when GST instead of GST-ctβARK was used, no $\beta\gamma$ dimer was detected in the pull-down assay (Fig. 2*B*). The quantification of three independent experiments shows no change (the decrease of the G$\beta\gamma$ recovery 25 s after stimulation was not statistically different from control condition) until 50 s after stimulation, when a 65 ± 9% increase in G$\beta\gamma$ recovery over the control value was evident, and it returned to control levels after 75 s (Fig. 2*C*). This result suggests that G protein may be activated by our stimulation protocol but also shows that the ctβARK binds G$\beta\gamma$ in our system, even in non-stimulated cells. This is a good control for the following experiments were this scavenger peptide was delivered by adenoviral transfection to block G$\beta\gamma$.

The $\beta\gamma$ Subunits Are Involved in Both PLC Activation and the Slow Calcium Signal Onset—The slow calcium signal induced by electrical stimulation was monitored in myotubes preloaded with Fluo-3AM. When myotubes were exposed to PTX, the slow calcium signal was strongly blocked (Fig. 3*A*); likewise, transfection with an adenovirus that encodes ctβARK (AdβARK) blocked the slow calcium signal (Fig. 3*B*). In contrast, the control transfection with an empty adenovirus (EV) showed no inhibitory effect (*control*, Fig. 3*B*).

To test the involvement of the G protein in PLC activation, IP_3 mass was measured as described under "Experimental Procedures." The IP_3 mass was measured 75 s after stimulation, because this is the time peak previously reported when the kinetics of IP_3 mass production was studied (14). The electrical stimulation generated an increase in IP_3 mass from 23 ± 6 in control conditions to 71 ± 10 pmol of IP_3/mg of protein (Fig. 3*C*). Pre-treatment with PTX blocked this IP_3 rise yielding 16 ± 2 pmol/mg of protein in the stimulated condition (Fig. 3*C*). In addition, in cultures transfected with an empty adenovirus (EV), electrical stimulation induced an increase in IP_3 mass from 29 ± 4 to 60 ± 7 pmol/mg of protein, whereas, in AdβARK-transfected cells, the IP_3 rise was inhibited (35 ± 5 pmol/mg of protein, Fig. 3*D*). Basal IP_3 values (~25 pmol/mg of protein) are fairly constant both in control cells and in those transfected with AdβARK or empty vectors. This may mean that G protein-dependent PLC is not the only isoform responsible for maintaining IP_3 levels.

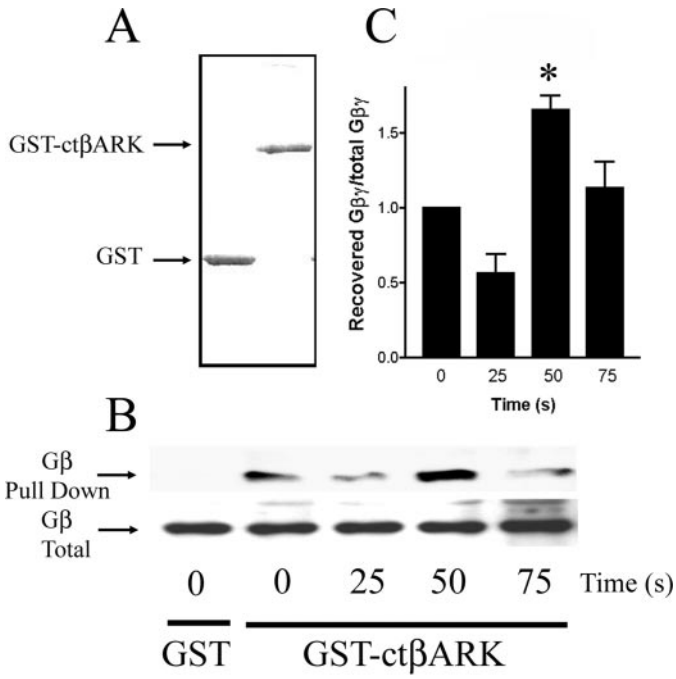

FIGURE 2. **The G protein is activated by the electrical stimulation.** Pull-down assay for G$\beta\gamma$ subunit was performed as describes under "Experimental Procedures." For this purpose, the GST fused to the carboxyl terminus of the β-adrenergic receptor kinase (GST-ctβARK) was expressed and purified (this protein has high affinity for G$\beta\gamma$) as a control was purified the GST (*A*). *B*, the stimulated lysates were exposed to the recombinant protein immobilized in glutathione-agarose resin, and the affinity-purified G$\beta\gamma$ from the lysates was subjected to Western blot developing using a monoclonal anti-Gβ antibody. Also, for each condition the total amount of Gβ was measured. *C*, the detected Gβ by the pull-down assay was corrected by the total Gβ of each condition and expressed *n*-fold over the control condition. The mean ± S.E. of three independent experiments is shown. The difference in the response is statistically significant; *, $p < 0.05$ *versus* control.

Electrical Stimulation Activates G$\beta\gamma$-dependent PI3K Activation—To measure PIP_3 production, myotubes were labeled with $^{32}PO_4$, and membrane lipids were extracted by chloroform and separated by TLC as described under "Experimental Procedures." Fig. 4*A* shows a representative result in which PIP_3 mass increased 40 s after stimulation. Incubation with wortmannin completely blocked PIP_3 formation. Upon electrical stimulation, PIP_3 mass increased transiently with a maximum of 74 ± 16% over control condition, 40 s after stimulation (Fig. 4*B*). To assess the participation of the G$\beta\gamma$ subunit, myotubes were transfected with either a control EV or an AdβARK construct. In controls, stimulation induced an increase of 98 ± 30% over the non-stimulated cells, whereas in AdβARK-transfected cells the stimulus did not generate any significant change in PIP_3 mass (Fig. 4*C*).

PI3K Is Involved in PLC Activation and the Slow Calcium Signal Onset—We tested the effect of wortmannin and LY294002 (LY), both inhibitors of PI3K, on the slow calcium signal and IP_3 mass production. Treatment with wortmannin strongly blocked the slow calcium signal

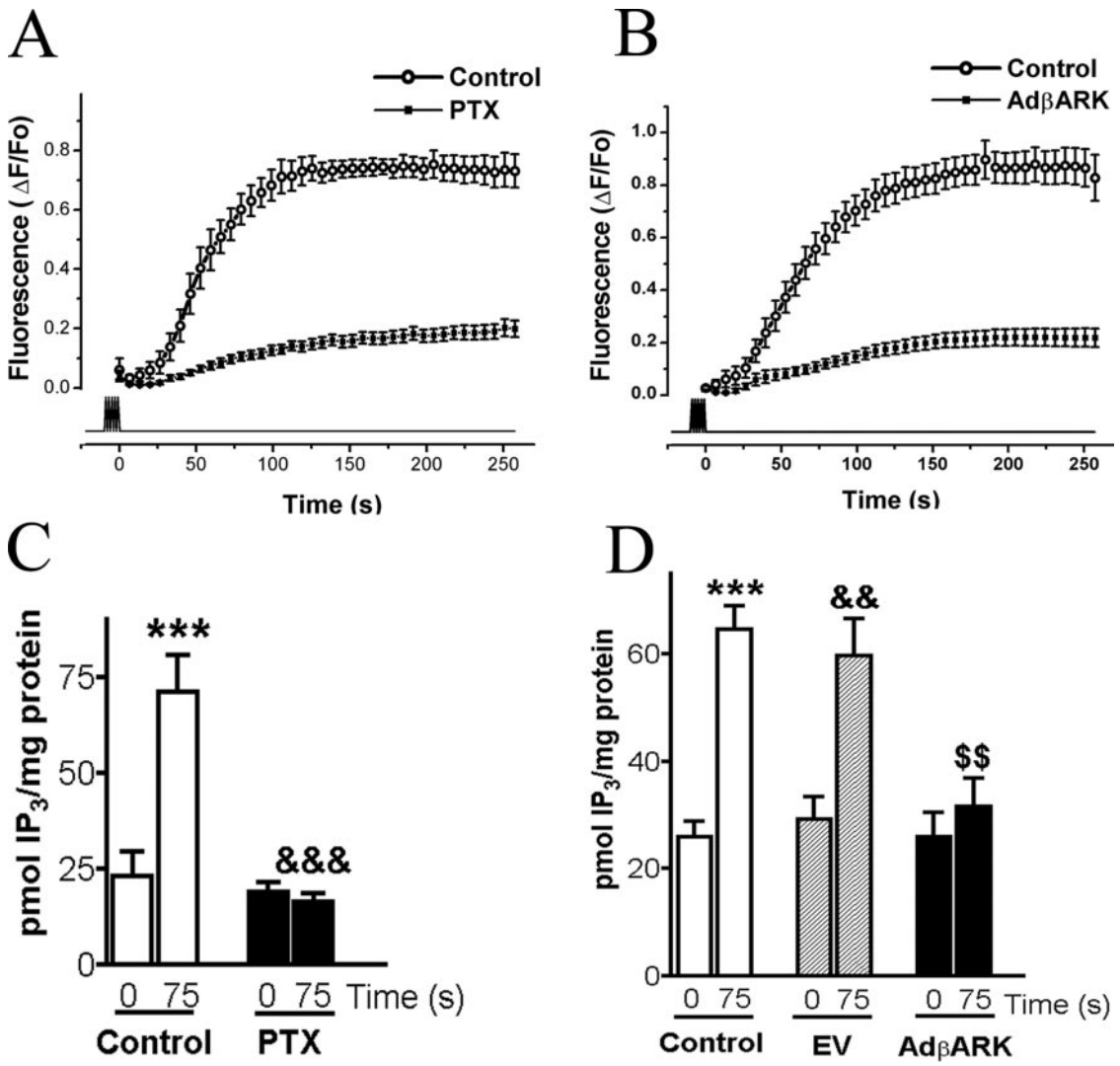

FIGURE 3. **Participation of G protein in the slow calcium signal induced by electrical stimulation.** *A*, the slow calcium signal induced by electrical stimulation (400 pulses of 1 ms at 45 Hz, *lower trace*) was measured in the presence of $G_{i/o}$ protein inhibitor pertussis toxin (*PTX*); the control condition in the absence of extracellular calcium (0.5 mM EGTA) is shown. The mean trace ± S.E. of at least 10 experiments is shown. *B*, the calcium signal was measured in myotubes transfected with an adenovirus that encodes the Gβγ scavenger ctβARK (*AdβARK*), and the controls were myotubes transfected with the empty adenovirus (*Control*) in calcium-free condition. The mean trace ± S.E. of at least 10 experiments is shown. *C*, the IP_3 mass was measured in myotubes 75 s after electrical stimulation (400 pulses of 1 ms at 45 Hz) in the presence and absence of PTX. The mean ± S.E. of three experiments is shown. IP_3 production induced by electrical stimulation (***, $p < 0.001$ *versus* corresponding control) was significantly inhibited by PTX treatment (&&&, $p < 0.001$ *versus* control stimulated condition). *D*, IP_3 measurement, 75 s after electrical stimulation in myotubes non-transfected (*Control*) or transfected alternatively with the empty adenovirus (*EV*) or AdβARK. The electrical stimulation induce an increase in IP_3 mass in the control condition (***, $p < 0.001$ *versus* corresponding control) and in EV transfection (&&, $p < 0.01$ *versus* corresponding control). The transfection of the Gβγ scavenger (*AdβARK*) strongly blocks the IP_3 production induced by the electrical stimulation ($$, $p < 0.01$ *versus* EV stimulated condition). The mean ± S.E. of five experiments is shown.

onset (Fig. 5*A*), and similar results were obtained when LY was used (data not shown). IP_3 mass induced by electrical stimulation was evaluated in cells exposed to LY or the vehicle (Me_2SO). In the presence of vehicle, the basal IP_3 mass was 27 ± 2 and increased to 76 ± 5 pmol of IP_3/mg of protein 75 s after the electrical stimulation. In the presence of LY, the electrical stimulation resulted in 25 ± 4 pmol of IP_3/mg of protein (Fig. 5*B*).

Similar experiments were done in the presence of wortmannin or the vehicle (Me_2SO). In the presence of the vehicle, electrical stimulation induced an increase of IP_3 mass from 20 ± 2 to 55 ± 6 pmol of IP_3/mg of protein. In the presence of wortmannin the stimulated condition was below basal (10 ± 1 pmol of IP_3/mg of protein) (Fig. 5*C*).

PI3Kγ Is Located Near the I-band Region of the Sarcomere, Displaying a Cross-striated Pattern—To define whether the p110γ isoform (the catalytic subunit of PI3Kγ) is expressed in cultured myotubes, Western blots of cell extracts were resolved by either mono- or polyclonal antibodies. In both cases, it displayed a single band at ~110 kDa (data not shown). To identify the subcellular localization of p110γ, skeletal myotubes were fixed and labeled for indirect immunofluorescence. As shown in Fig. 6 (*A* and *B*, *center panel*), a cross-striated pattern suggesting sarcomeric or a T-tubular system localization was clearly seen. To assess the location in more detail, the p110γ was simultaneously labeled with an A-band or a Z-line marker (myosin or α-actinin, respectively). Myosin label (Fig. 6*A*, *upper panel*) shows a regular dotted pattern, which corresponds to striations of the A-band of the sarcomere. The gaps within the staining correspond to I-band. Although in the merged image (Fig. 6*A*, *lower panel*), a slight co-localization is seen (*yellow dots*) the main p110γ staining is located in the gaps between the myosin staining, suggesting that p110γ is located in the I-band region. On the other hand, α-actinin, which runs along the center of the I-band, shows a higher co-localization pattern with p110γ stain (Fig. 6*B*, *lower panel*), supporting the idea that this PI3K isoform is located in the I-band region

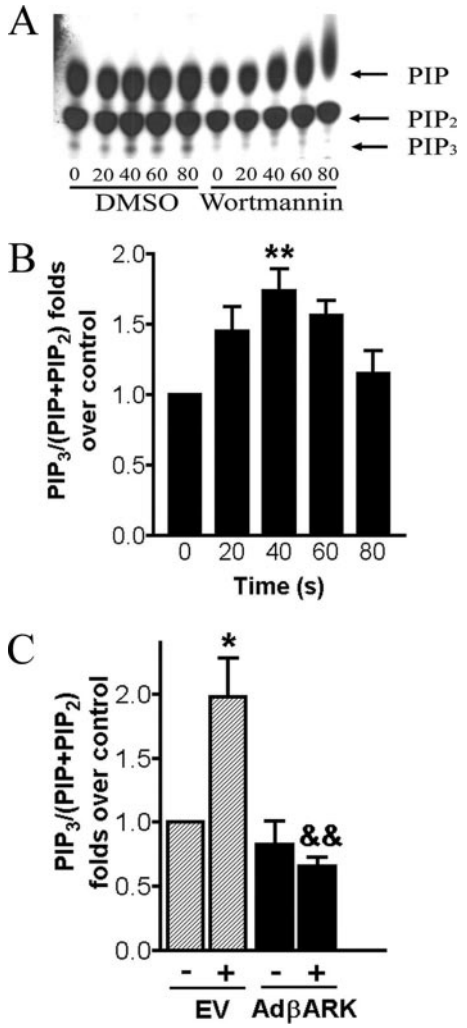

FIGURE 4. **Activation of PI3K by electrical stimulation.** Myotubes were labeled with $^{32}PO_4$, after the stimulation the phospholipids were isolated by chloroform extraction and subjected to TLC to separate the PIPs. The experiments were performed in the presence of wortmannin or the vehicle, Me_2SO. *A*, a representative experiment showing PIP, PIP_2, and PIP_3 after the indicated time post electrical stimulation (400 pulses of 1 ms at 45 Hz). *B*, the transient increase in PIP_3 after stimulation is shown; mean ± S.E. of five experiments is shown (**, $p < 0.01$ *versus* control). *C*, the production of PIP_3 induced in control (−) or 40 s after electrical stimulation (+) was measured in myotubes transfected with an empty adenovirus (*EV*) (*, $p < 0.05$ *versus* corresponding control) or transfected with an adenovirus that encodes the Gβγ scavenger βARK (*AdβARK*). The transfection of AdβARK strongly blocks the PIP_3 production induced by electrical stimulation ($^{\&\&}$, $p <$ 0.01 *versus* EV stimulated condition). The mean ± S.E. of three experiments is shown.

of the sarcomere. The T-tubule, where the DHPR is placed, runs near the I-A band junction of the sarcomere. The co-localization image between the DHPR and p110γ (Fig. 6*C*, *upper panel*) clearly shows that the bulk stain of both markers do not co-localize but are located in two structures that are close one another. A magnification of the image reveals that both structures have discrete points of co-localization (Fig. 6*C*, *lower panel*, *arrow* indicated *yellow dots*). To visualize such co-localization areas of the image, the single images of p110γ and DHPR staining were operated to visualize the pixels where the co-localization takes place (Fig. 6*C*, *center panel*). The image shows that the co-localization dots are widely distributed over the myotube.

PI3Kγ Is Activated by Electrical Stimulation—The PH domain of the BTK fused to enhanced GFP had been described as a probe for PIP_3, because of its high affinity for this particular phospholipid (15). Primary cultured myotubes were transfected with (PH)BTK-GFP to measure PIP_3 production in the absence of extracellular calcium after electrical

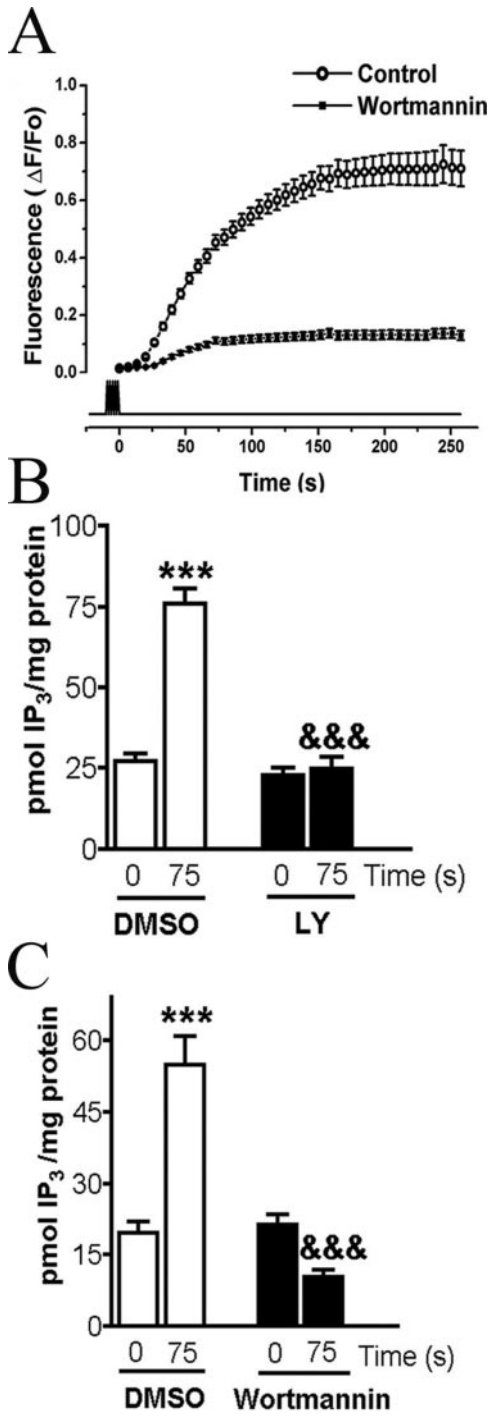

FIGURE 5. **Participation of PI3K in the slow calcium signal induced by electrical stimulation.** *A*, the slow calcium signal induced by electrical stimulation (400 pulses of 1 ms at 45 Hz) was measured in presence of PI3K inhibitor (wortmannin) or the vehicle (control) in the absence of extracellular calcium (0.5 mM EGTA). The mean trace ± S.E. of at least 10 experiments is shown. *B*, the IP_3 mass was measured in myotubes 75 s after the electrical stimulation in presence of the vehicle (Me_2SO) or LY294002 (LY). The mean ± S.E. of five experiments is shown. The production of IP_3 induced by electrical stimulation (***, $p < 0.001$ *versus* the corresponding control) was significantly inhibited by LY treatment ($^{\&\&\&}$, $p < 0.001$ *versus* the stimulated Me_2SO condition). *C*, the IP_3 production induced 75 s after the electrical stimulation was measured in myotubes in presence of the vehicle (Me_2SO) or wortmannin. The production of IP_3 induced by electrical stimulation (***, $p < 0.001$ *versus* the corresponding control) was significantly inhibited by wortmannin treatment ($^{\&\&\&}$, $p < 0.001$ *versus* the stimulated Me_2SO condition). The mean ± S.E. of six experiments is shown.

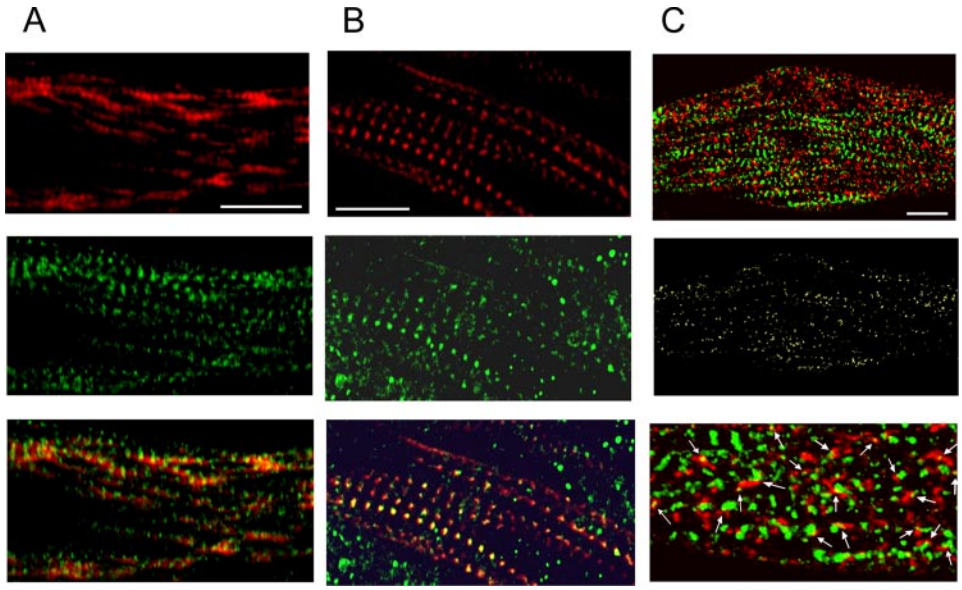

FIGURE 6. **PI3Kγ is localized in the I-band of myotubes.** *A*, confocal images of a single optical section (<0.5 μm) of a myotube, showing the A-band marker myosin in *red* (*upper panel*), p110γ immunostaining in *green* (*center panel*), and merge of both images (*lower panel*). *Scale bar*, 10 μm. *B*, co-localization of the Z-line marker α-actinin and p110γ in a confocal image of a single section (<0.5 μm) showing immunostained α-actinin in *red* (*upper panel*) with the immunostained p110γ in *green* (*center panel*) and the merge of both images (*lower panel*). Notice the co-localization as overlay of both colors (*yellow*). *Scale bar*, 10 μm. *C*, a fused confocal image of a single optical section (<0.5 μm) of a myotube, showing p110γ immunofluorescence in *green* and DHPR (T-tubule marker) in *red* (*upper panel*); *scale bar*, 10 μm. The *center panel* shows an image of the fraction of pixels that have only *green* and *red* staining (in *yellow*) of the whole image shown in the *upper panel*. The *lower panel* shows a digital zoom of the *upper panel image*, co-localization *dots* (*yellow*) are marked by *arrows*.

stimulation in single living cells. At rest, the fluorescent probe was visualized both in cytosol and nuclei (Fig. 7*A*). The quantification of the pixel intensity of the *line that crosses the myotube* depicted in Fig. 7*A* also shows a homogeneous pattern. A few seconds after electrical stimulation (7–14 s) a progressive decrease of fluorescent intensity started and reached the lowest level (50% of the initial fluorescence) 2 min after the stimulus ended (Fig. 7, *B* and *G*). Over the following minutes, the fluorescence intensity of the optical section increased, while the probe migrated to the plasma membrane showing a clear membrane location as seen by the quantification of the pixel intensity of the *line that crosses the myotube* (Fig. 7*C*). The exposure of the cells to 100 nM wortmannin completely abolished the fluorescence fluctuation as well as the fluorescent protein migration (Fig. 7, *D*–*G*).

Cultured dyspedic cells (1B5 skeletal muscle cell line) were transfected with (PH)BTK-GFP to measure PIP_3 production after the electrical stimulation. 1B5 cells were used because they lack expression of all forms of ryanodine receptor, so calcium is not released during stimulation avoiding possible artifacts due to cell contraction. As seen for primary culture, few seconds after electrical stimulation, fluorescence in the confocal plane transiently decreased as shown in Fig. 7*H*. This result suggests that the probe changes its subcellular location after the stimuli, probably due to PIP_3 formation. As controls, 1B5 cultures were transfected with either a point mutated PH domain (R28C) fused to enhanced GFP that is unable to bind PIP_3 ((PHmut)BTK-GFP) or with the enhanced GFP alone (GFP). In neither case did the stimulation induce an effect similar to the one observed with the (PH)BTK-GFP probe, suggesting that it is specific to the functional PH domain linked to the enhanced GFP (Fig. 7*H*). To assess the participation of the PI3Kγ isoform in PIP_3 production, the (PH)BTK-GFP probe was co-transfected with either a kinase-inactive version of the PI3Kγ (KR), with the wild-type (wt) PI3Kγ or with the probe alone (Fig. 7*I*). Co-transfection of PI3Kγ(KR) strongly inhibited the transient decrease of the probe fluorescence induced by electrical stimulation; on the other hand, transfection with the PI3Kγ(wt) did not show any difference with the control condition (Fig. 7*I*). When primary cultured myotubes were co-transfected with the (PH)BTK-GFP probe and the PI3Kγ wt or the PI3Kγ (KR), the transient decrease in fluorescence induced by electrical stimulation was abolished only when the kinase inactive PI3Kγ was expressed (Fig. 7*J*). Primary myotubes were also co-transfected with the (PH)BTK-GFP and the membrane targeted CAA*X*-PI3Kγ wt or the membrane targeted kinase inactive CAA*X*-PI3Kγ (KR). Only the kinase inactive PI3Kγ form strongly inhibited the transient decrease of the probe fluorescence (Fig. 7*K*).

PI3Kγ Is Involved in the Slow Calcium Signal Onset—To test the participation of PI3Kγ in the progression of the slow calcium signal, primary cultured myotubes were co-transfected with a red fluorescent protein (DsRed) as transfection marker and wt or (KR) PI3Kγ variant. The calcium signal was measured with Fluo3 as described under "Experimental Procedures." When cells were transfected only with DsRed (control) or co-transfected with the PI3Kγ wt, the myotubes showed a similar slow calcium signal response to electrical stimulation. Overexpression of the kinase inactive PI3Kγ (KR), on the other hand, strongly diminished the slow calcium signal induced by the electrical protocol (Fig. 8*A*). Similarly, when the membrane-targeted CAA*X*-PI3Kγ wt was used, a clear signal was obtained and when membrane-targeted CAA*X*-PI3Kγ (KR) variants were used, stimulation resulted in a much smaller signal (Fig. 8*B*).

Electrical Stimulation Induced PLCγ1 Phosphorylation in Myotubes—Cultured myotubes were electrically stimulated (400 1-ms pulses at 45 Hz). After the indicated periods of time, the cultures were extracted, and Western blot assays were performed to assess the kinetics of PLCγ1 phosphorylation. A representative experiment of PLCγ1 phosphorylation kinetics for each condition after electrical stimulation is shown (Fig. 9*A*). The quantification of the ratio between pPLCγ1/PLC in a total of five experiments shows a 3-fold increase 30 s after stimulus (2.97 ± 0.28-fold over non-stimulated control). Between 40 and 50 s after stimulus, phosphorylation increased only 40% over control (1.39 ± 0.2 and 1.38 ± 0.32-fold over control, respectively). Finally, 70 s after stimulation phosphorylation is similar to control condition (0.93 ± 0.21-fold over control). To investigate the subcellular location in which PLCγ is phosphorylated, cells were cultured on coverslips and double-stained with both anti-pPLCγ1 and anti-total PLCγ1 primary antibodies (Fig. 9*B*). In non-stimulated cells, PLCγ1 phosphorylation was seen as a slight label with a diffuse pattern in the cytoplasm, whereas total PLCγ1 is present both in the cytoplasm and in the plasma membrane. However, after stimulation (Fig. 9*B*), the pPLCγ1 stain increased and located both in the nuclear envelope and diffusely in the cytoplasm. The total PLCγ1 label shows again a diffuse pattern in cytoplasm. The merge between phosphorylated and total PLCγ1 images co-localized in cytoplasm regions (Fig. 9*B*). These results suggest that phosphorylation of PLCγ1

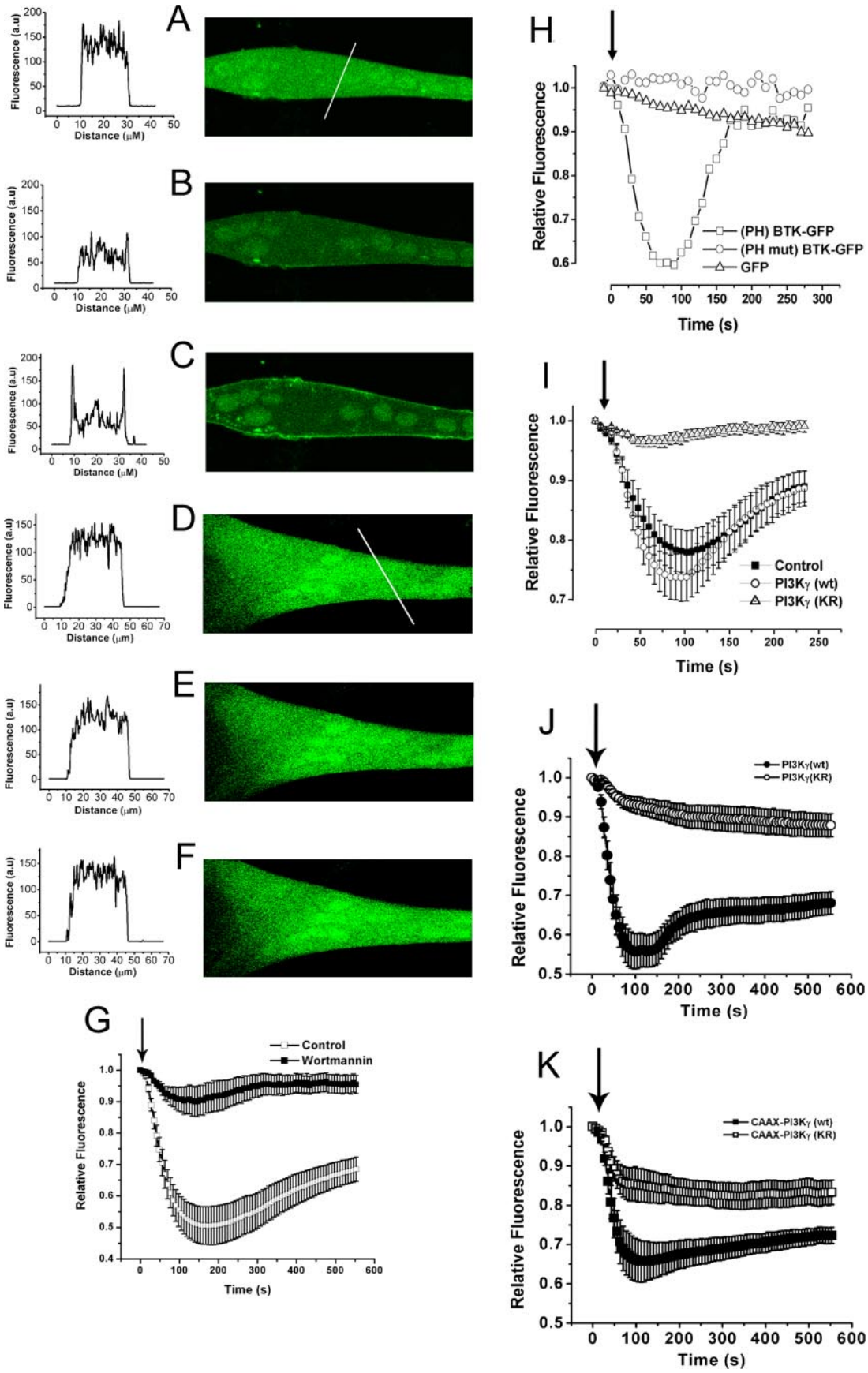

FIGURE 7. **Measurement of PIP_3 induced by electrical stimulation in single live myotubes.** The fluorescent images of a myotube transfected with a fusion protein between the PH domain of BTK and the enhanced GFP were acquired by confocal microscopy every 7 s, and the *arrow* indicates the start of the electrical stimulation (400 pulses of 1 ms at 45 Hz; the stimulation lasted for 9 s). *A*, fluorescent image before stimulation (*right*); pixel intensities along the *line across the myotube* are plotted (*left*). *B*, fluorescent image 120 s after

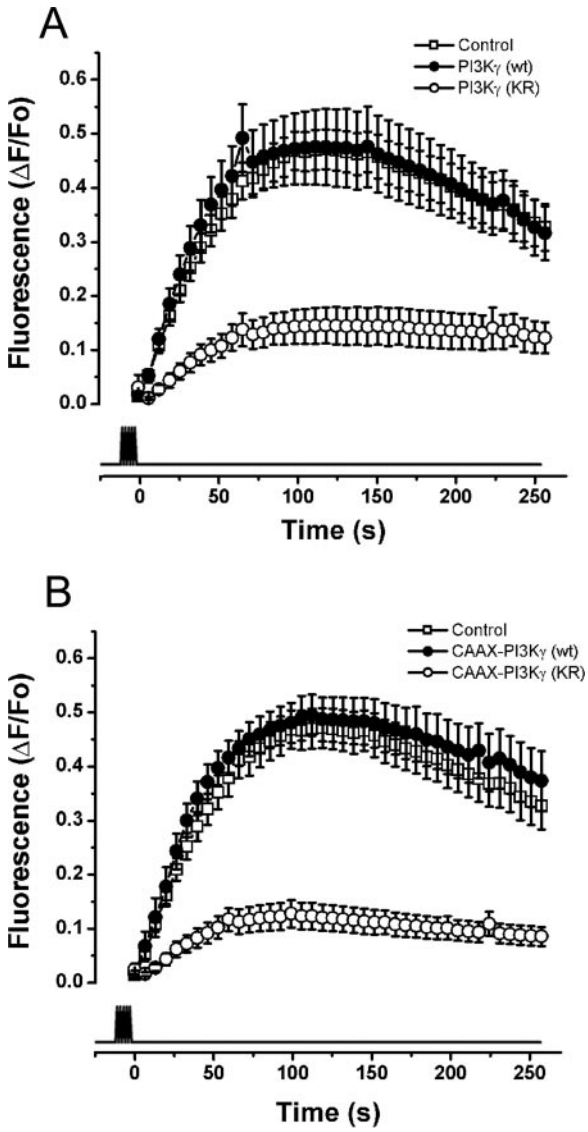

FIGURE 8. **Participation of PI3Kγ in the slow calcium signal induced by electrical stimulation.** The slow calcium signal induced by electrical stimulation (400 pulses of 1 ms at 45 Hz, *lower trace*) was measured in myotubes co-transfected with wild type (*wt*) or the kinase inactive (*KR*) variant of PI3Kγ and the monomeric red fluorescent protein (DsRed) as transfection marker in the absence of extracellular calcium (0.5 mM EGTA). *A*, cells transfected with DsRed as control (*Control*), or co-transfected with DsRed plus PI3K wt or DsRed plus PI3K (KR). *B*, cells co-transfected with DsRed and the membrane-targeted CAA*X*-PI3K (wt) or CAA*X*-PI3K (KR). The mean trace ± S.E. of at least 12 experiments is shown.

after electrical stimulation occurs in the cytoplasm and not in the plasma membrane.

A Fraction of the Phosphorylated PLCγ1 Was Located in the Nuclear Envelope—For a precise subcellular localization of phosphorylated PLCγ1, cells were double-stained with anti-pPLCγ1 and anti-LAP 2 primary antibodies (LAP 2 is an inner nuclear membrane marker). Fig. 9*C* shows phosphorylation of PLCγ1 in a control, non-stimulated myotube, in which a diffuse pattern of a low intensity staining is observed. The LAP2 antibody clearly stained the nuclear envelope. Electrical stimulation of the cells induced phosphorylation of PLCγ1 both in the cytosol and in the nuclear envelope. The overlap of the pPLCγ1 and LAP2 images clearly shows the co-localization of both stains suggesting that at least a fraction of the phosphorylation process occurred in the inner nuclear membrane region (yellow, Fig. 9*C*).

DISCUSSION

Studies on voltage-gated ion channels in excitable cells have naturally focused on their ion permeation and gating properties; we focused on a new property for an L-type Ca^{2+} voltage-gated channel, *i.e.* to act as a voltage sensor for a G protein-regulated signal involving activation of PI3K and PLC. At present, little information exists about signaling pathways activated by conformational changes of voltage-gated channels. One example is the skeletal muscle EC coupling model, where there is bi-directional cross-talk between the DHPR and the ryanodine receptor, independently of the calcium channel function of the former (24, 25). Our laboratory has shown that membrane depolarization obtained by either high potassium or tetanic electrical stimulation induces PLC activation followed by an IP_3-dependent slow calcium signal (5, 14). Absence of extracellular calcium does not affect slow calcium signal progression, whereas treatment with an agonist dihydropyridine (Bay K8644) in the absence of external calcium accelerates it. Transfection with the α1S subunit cDNA of the DHPR (the voltage sensor and pore forming subunit of the channel) in myotubes that lack α1S rescues the slow calcium signal (6, 14). These results suggest that action potentials activated by electrical stimulation may induce conformational transitions of DHPR that, independently of its calcium channel properties, set in motion signaling pathways involved in PLC activation.

We used an external electrical field to generate action potentials, so it allowed us to cycle the DHPR through its voltage-dependent conformational states; this stimulus pattern will partly mimic the physiological motor unit activity. The action potential as stimulus for the slow calcium signal was confirmed by blocking the voltage-gated sodium channels with tetrodotoxin (14). To better characterize our stimulation protocol, we measured the action potentials induced by the electrical field at different frequencies. Spontaneous action potentials last 33 ms, so the prediction would be that the cell may be unable to elicit all action potentials for each stimulation pulse at 45 Hz (22 ms between pulses). As shown in Fig. 1*F*, cells accelerate the repolarization rate reaching 15-ms action potential duration at 45 Hz, allowing one action potential for each pulse of the train. This rate increase may be explained by enhanced chloride and potassium conductances activated by the calcium increase (26, 27) during the electrical stimulation shown in Fig. 1*B*. The time course of progression of the slow calcium signal in the single cell depicted in Fig. 1*D* shows some differences with the mean control signals shown in Figs. 3*A*, 3*B*, and 5*A*. The former was measured in

stimulation (*right*); pixel intensities along the *line* are plotted (*left*). *C*, fluorescent image 9 min after stimulation (*right*); the quantification of pixels intensities of the *line* is plotted (*left*). *D–F* show the same objects as in *A–C*, respectively, but in the presence of wortmannin. *G*, the kinetics of fluorescence intensity of the whole cell after stimulation is plotted for control and wortmannin-treated cells. The mean trace ± S.E. of at least 10 experiments is shown. *H*, myotubes from 1B5 cells were transfected with a fusion protein between the PH domain of BTK and the enhanced GFP ((PH)BTK-GFP); this probe has high affinity for PIP_3. As control, a probe that has a mutation on the PH domain (R28C) that abolishes the affinity for PIP_3 was used. The kinetics of the fluorescent intensity for these cells as well as for a control cell transfected with enhanced GFP alone is shown. All experiments were performed in the absence of extracellular calcium. *I*, myotubes from 1B5 cells were transfected with (PH)BTK-GFP alone (*Control*), or co-transfected with kinase defective PI3Kγ (*PI3Kγ(KR)*) or a PI3Kγ wild type (*PI3K(wt)*). Only the dominant negative variant of PI3Kγ blocked the PIP_3 signal induced by electrical stimulation. Images were acquired every 6 s. The mean trace ± S.E. of at least 14 experiments is shown. *J*, PIP_3 was measured in primary cultured myotubes transfected with (PH)BTK-GFP and subjected to electrical stimulation (400 pulses of 1 ms at 45 Hz, indicated by the *arrow*). This fluorescent tracer was co-transfected with wild type (*wt*) or the kinase inactive (*KR*) variants of PI3Kγ in the absence of extra cellular calcium (0.5 mM EGTA). *K*, PIP_3 kinetics in cells co-transfected with the PH-GFP probe and the membrane-targeted CAA*X*-PI3K (wt) or CAA*X*-PI3K (KR). The mean trace ± S.E. of at least 10 experiments is shown.

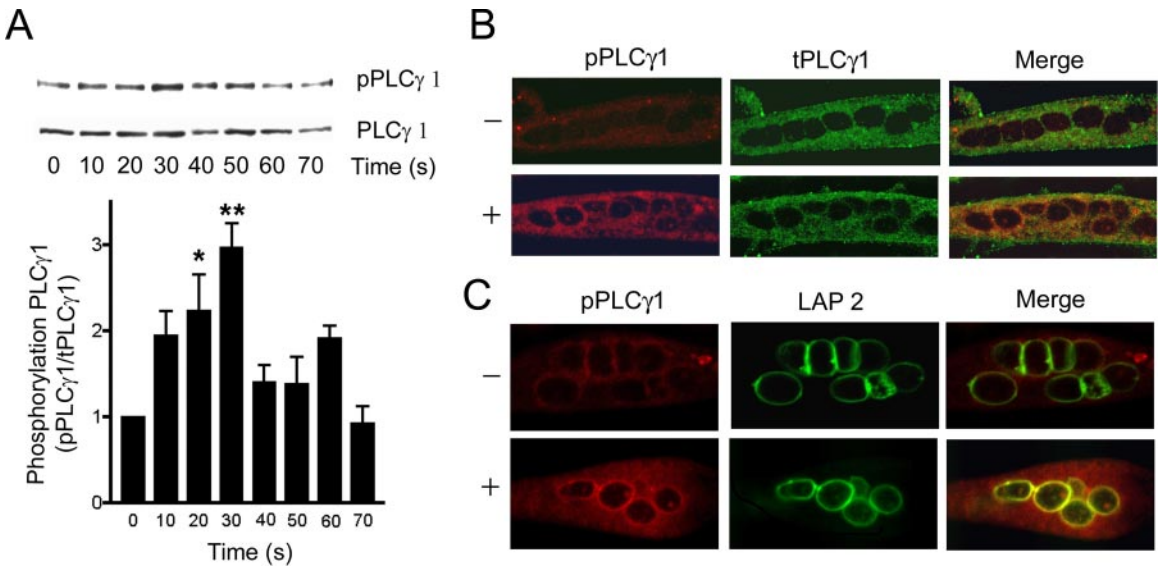

FIGURE 9. **Electrical stimulation induce PLCγ1 phosphorylation in myotubes.** Cultured myotubes were electrically stimulated (400 pulses of 1 ms at 45 Hz). *A*, representative Western blot of PLCγ1 phosphorylation kinetics (*above*) and total amount of PLCγ1 (*below*) are shown. The ratio between phosphorylated PLCγ1 (*pPLCγ1*) and the total amount of PLCγ1 is shown. The maximal increase in phosphorylation was 30 s after stimulus (**, $p < 0.01$ *versus* non-stimulated control). Mean ± S.E. of 5 experiments is shown. *B*, PLCγ1 phosphorylation after electrical stimulation was evaluated by immunofluorescence. Cells were double-stained with anti-pPLCγ1 and total PLCγ1 primary antibodies and secondary antibodies used were conjugated with Alexa 633 and Alexa 488, respectively. Control non-stimulated cells (−) and electrical stimulated cells (+) are shown. pPLCγ1 is depicted in *red* (*left*) and total PLCγ1 in *green* (*center*), and the merge of both images is shown (*right*). The merged image in the stimulated condition shows co-localization in cytoplasm; no co-localization was detected in the plasma membrane. *C*, to study in more detail the nuclear location of PLCγ1 phosphorylation, non-stimulated (−) and stimulated cells (+) were double-immunostained with anti-pPLCγ1 and anti-Lap 2 primary antibodies. The secondary antibodies used were conjugated to Alexa 633 and Alexa 488, respectively. pPLCγ1 staining is depicted in *red* (*left*) and Lap 2 is in *green* (*center*). The *right image* is the merge between both images. The stimulated condition shows co-localization in the perinuclear region (*yellow*).

medium containing calcium, whereas the later was done in calcium-free medium. As previously published, the absence of extracellular calcium delays the signal progression, probably by an initial entrance of calcium ions (14).

The onset of the slow calcium signal, induced by tetanic stimulation (400 1-ms pulses at 45 Hz), has a 30- to 40-s delay after the end of stimulation (14). This observation suggests that a signaling pathway must be activated during this period. There is scant evidence in the literature for G protein activation induced by cell depolarization. Cohen-Armon and co-workers have described in synaptoneurosomes (vesicles that contain presynaptic and postsynaptic sac) that depolarization induces activation of PTX-sensitive G proteins; in particular, they describe the activation of $G\alpha_{o1}$ and $G\alpha_{o3}$ isoforms. Interestingly when they prevented activation of voltage-gated sodium channels using DPI 201–106 R enantiomer, they abolished G_o protein activation. In contrast, treatment with tetrodotoxin did not have any effect, consistent with a conformational rather than a Na^+ current dependent-mechanism for G protein activation (28, 29). As described above, in our system we have demonstrated that $\alpha 1_S$ is critical for the depolarization-induced PLC activation, involving the participation of a PTX-sensitive G protein. Together, these observations suggest that depolarization-induced G protein activation may be a conserved mechanism for some voltage-gated channels.

In particular, L-type channels (DHPRs) have not been reported to be directly modulated by G proteins, nor had a direct interaction between DHPR and a heterotrimeric G protein been described. Nevertheless, in adult muscle, co-localization of DHPR and G_o proteins in the T-tubule membrane was described (33), the G protein being found in purified T tubular membranes. On the other hand, other types of voltage-gated calcium channels (P/Q- and N-type), not expressed in skeletal muscle, have binding sites for $G\beta\gamma$. The G protein has an inhibitory role due to a positive shift in the voltage dependence and a slowing of channel activation; these effects are relieved by strong depolarization resulting in a facilitation of Ca^{2+} currents (30–32). The phenomenon that we are describing here suggests that, unlike what has been described for other calcium channels, the DHPR conformational transitions may be activating the G protein; biochemical studies should be addressed to define the possible physical interaction between DHPRs and G proteins in the future.

The pull-down assay performed (Fig. 2*C*) shows that 50 s after stimulation, $G\beta\gamma$ protein recovery was increased over the control condition, suggesting increased release of free-$G\beta\gamma$ protein. These free $G\beta\gamma$ protein fluctuations in turn suggest an early G protein activation upon electrical stimulation. Unfortunately the pull-down assay described here is unable to measure the G protein activation during the electrical stimulation protocol, so it is necessary to develop a single cell method for G protein activation *in vivo* to address this point in the future.

Two different experimental approaches suggest that G protein activation be involved in PLC activation. First, the exposure to PTX and second, adenoviral transfection of ctβARK. Both procedures almost completely blocked both the slow calcium signal and the IP_3 transient induced by tetanic stimulation (Fig. 3). These results suggest the participation of $G\beta\gamma$ from a PTX-sensitive G protein in PLC activation. $G\alpha_o$ (sensitive to PTX) and $G\beta$ have been detected as a dotted pattern evoking triadic structure repetition in adult skeletal muscle (33). Furthermore, Western blot analysis against $G\alpha_{i/o}$ isoforms in a highly purified T-tubule preparation from adult skeletal muscle revealed that at least $G\alpha_{i2}$, $G\alpha_{i3}$, and $G\alpha_o$ are present, all of these being susceptible to PTX-mediated ADP-ribosylation (34). As described above, both the IP_3 transient and slow calcium signal induced by electrical stimulation depend on DHPR and on a PTX-sensitive G protein. The common subcellular location (T-tubule) of both proteins is in agreement with their possible role in the signaling pathway outlined in this work, where DHPR acts as voltage sensor and the G protein as the transductor involved in effector (PLC) activation.

At least two ways how $G\beta\gamma$ subunit may mediate PLC activation have

been described in the literature. Either $G\beta\gamma$ interacts with the PH domain of PLCβ acting as an allosteric site for the activation of the catalytic core of the protein (35, 36) or $G\beta\gamma$ may activate the PI3Kγ, which catalyzes the phosphorylation of phosphatidylinositol 4,5-bisphosphate (PIP_2) in the D3 position of the inositol ring yielding PIP_3. The latter is a known second messenger involved in membrane recruitment of PLCγ, where it is activated after tyrosine phosphorylation (12, 13). Within this context, we evaluated the participation of PI3K as part of this transduction mechanism, and we measured PIP_3 production after tetanus. Indeed we found an increase in PIP_3 40 s after tetanic electrical stimulation (Fig. 4). In addition, viral transfection of ctβARK abolished PIP_3 production. To further evaluate whether PI3K is involved in PLC activation induced by electrical stimulation, we exposed myotubes to PI3K inhibitors. Both LY and wortmannin completely blocked both the slow calcium signal and the IP_3 mass transient increase induced by the electrical stimulation (Fig. 5). These results, together with the fact that PI3Kγ is known to be activated by the $G\beta\gamma$ subunit (37, 38), suggest that PI3Kγ is a good candidate for PIP_3 production.

Little evidence on PI3Kγ in skeletal muscle is currently available, but the development of a transgenic mice defective in PI3Kγ (PI3K$\gamma^{-/-}$) has provided some clues on the possible physiological role of PI3Kγ in others tissues. Several studies describing the role of this kinase in inflammation (39) suggest that it is a potential pharmacological target for chronic inflammation and allergies (40). PI3K$\gamma^{-/-}$ mice show basal enhancement of cardiac contractility and exposure to pressure overload of the left ventricle rapidly develops into signs of chamber dilation and dysfunction (41). Smooth muscle cells require PI3Kγ for angiotensin II-mediated intracellular Ca^{2+} increase, through an L-type channel-dependent mechanism, favoring smooth muscle contraction (42). In addition, vessels of PI3K$^{-/-}$ mice show reduced contractile response to angiotensin II (43). PIP_3 production by the $G\beta\gamma$/PI3Kγ pathway and the subsequent protein kinase C activation were suggested to be responsible of these angiotensin II effects (44, 45).

Although the presence of PI3Kγ mRNA in skeletal muscle was reported 10 years ago (37), its physiological role has not been elucidated. We confirmed its presence in myotubes by Western blot using two different antibodies (data not shown). The double-labeling immunofluorescence studies indicate a very mild co-localization of PI3Kγ with the A-band marker myosin and a strong co-localization with the Z-line marker α-actinin, consistent with an I-Band location of the enzyme at rest. These results suggest that PI3Kγ could be located in a structure near the longitudinal sarcoplasmic reticulum membrane besides the triad. In agreement with that interpretation, DHPR clusters marking the T-tubule membrane (46) of triad are found in the region of the A-I band interface, and the PI3Kγ shows a partial co-localization with the DHPR suggesting that the bulk of PI3Kγ is located in the I-band (near to the sarcoplasmic reticulum) and only a small fraction of the protein is closer to the T-tubule in the I-A junction. These findings suggest that PI3Kγ could be near the T-tubule. It is possible then, that after electrical stimulation, the DHPR acting as voltage sensor may activate $G\beta\gamma$, which in turn will activate PI3Kγ, which in turn will translocate to the T-tubule where most of the mass of PIP_2 (PI3K substrate) is found (47).

To visualize the changes in PIP_3 in living cells, primary myotubes and dyspedic cells (1B5) were transfected with a plasmid encoding (PH)BTK-GFP. This PH domain binds selectively PIP_3, both *in vitro* and *in vivo* (15, 18). When this probe was transfected in NIH 3T3 cells, fluorescence was located diffusely in both the nuclei and cytosol, and after PDGF treatment, fluorescence was redistributed decreasing in cytosol and increasing in the plasma membrane (15). Unlike most cells, skeletal muscle cells show an unusual intracellular membrane architecture where the membrane surface in the T-tubule is much larger than in the plasma membrane. Because our data suggest that PIP_3 formation is likely to occur in the T-tubule, the (PH)BTK-GFP probe would be expected to move toward the T-tubule. When transfected primary myotubes were stimulated, the first 2 min after stimulation the probe, rather than concentrate in a striated pattern, transiently disappeared and then progressively started to reappear in the plasma membrane. Both behaviors of the probe after electrical stimulation were abolished by wortmannin. These results suggest that at least two events are occurring; first the probe could either be rapidly redistributed after stimulation, so fluorescence decreases in the confocal plane, and/or the T-tubule environment quenches the enhanced GFP fluorescence. Second, a late PIP_3 production by the activation of a PI3K isoform (other than γ) in the plasma membrane could explain the migration of the probe to the plasma membrane. When (PH)BTK-GFP-transfected dyspedic (1B5) myotubes were electrically stimulated, the cells only displayed the first response (transient decrease of the probe fluorescence), and the late migration to the plasma membrane was absent. This finding, in addition to the fact that these cells show a slow calcium response after electrical stimulation (14), suggests that the initial PIP_3 production is enough to elicit PLC activation. Transfection of a mutated probe (that does not bind PIP_3) or of GFP without a fused PH domain did not show the transient decrease in fluorescence, supporting the idea that this response is specific for this functional PH domain. The transient decrease of fluorescence induced by electrical stimulation was blocked by the kinase-inactive variant of the PI3Kγ, whereas the co-transfection of PI3Kγ(wt) did not show any difference with the control condition. These results suggest that PI3Kγ is indeed the isoform activated by electrical stimulation.

When primary myotubes were co-transfected with the kinase-inactive variant of PI3Kγ, the first response (transient decrease of fluorescence) was completely blocked, whereas in some cells the late plasma membrane translocation of the probe was still present (data not shown), suggesting that PI3Kγ is mainly involved in the first response. When membrane-targeted (CAA*X*) PI3Kγ wt and (KR) kinase-inactive variants were co-transfected with the (PH)BTK-GFP, results similar to those using non-targeted PI3Kγ were obtained, suggesting that the membrane location does not give any advantage to the dominant negative variant of PI3Kγ. This could be explained assuming that the non-membrane targeted protein (without CAA*X*) has enough targeting information to localize in the place where transduction takes place (probably the co-localization dots between DHPR and PI3Kγ in the T-tubule, Fig. 6*C*). The slow calcium signal was strongly inhibited in cells transfected with either PI3Kγ (KR) or membrane-targeted CAA*X*-PI3Kγ (KR), whereas wt variants did not show any difference with the control condition. These results suggest that the early production of PIP_3 by PI3Kγ is essential for the activation of PLC and the slow calcium signal progression. Further studies should be addressed to reveal the role of the putative late PIP_3 production in the plasma membrane after electrical stimulation.

In agreement with the hypothesis of an early PIP_3 generation being responsible for PLC activation, the maximum levels of PLCγ1 phosphorylation induced by electrical stimulation was reached 30 s after the stimulus ended. These kinetics fit with the quick reduction of fluorescence of the (PH)BTK-GFP probe after stimulation. In addition, despite of the basal presence of PLCγ1 in the plasma membrane, the fraction that is phosphorylated after electrical stimulation is in the cytosol and the nuclear envelope region, suggesting that at least part of the phosphorylation could be occurring in intracellular membranes. Both the T-tubule membrane and the nuclear envelope are candidates for such a role.

In summary, our data provide novel evidence to support the notion

that electrical stimulation induces activation of the Gβγ/PI3Kγ pathway mediating both PLC activation and the slow calcium signal. The DHPR/G protein mechanism outlined here opens new perspectives for the study of signaling processes, because electrical fluctuations of the cell membrane can be translated not only into well known fast responses but also into a message for the activation of signaling pathways that may modulate long term adaptive responses.

Acknowledgments—We thank Dr. Paul D. Allen (Brigham and Women's Hospital, Boston, MA) for helpful discussions and for providing the 1B5 cells and Mónica Silva for cell cultures and transfection.

REFERENCES

1. Tanabe, T., Beam, K. G., Adams, B. A., Niidome, T., and Numa, S. (1990) *Nature* **346,** 567–569
2. Grabner, M., Dirksen, R. T., Suda, N., and Beam, K. G. (1999) *J. Biol. Chem.* **274,** 21913–21919
3. Protasi, F., Paolini, C., Nakai, J., Beam, K. G., Franzini-Armstrong, C., and Allen, P. D. (2002) *Biophys. J.* **83,** 3230–3244
4. Proenza, C., O'Brien, J., Nakai, J., Mukherjee, S., Allen, P. D., and Beam, K. G. (2002) *J. Biol. Chem.* **277,** 6530–6535
5. Jaimovich, E., Reyes, R., Liberona, J. L., and Powell, J. A. (2000) *Am. J. Physiol.* **278,** C998–C1010
6. Araya, R., Liberona, J. L., Cardenas, J. C., Riveros, N., Estrada, M., Powell, J. A., Carrasco, A., and Jaimovich, E. (2003) *J. Gen. Physiol.* **121,** 3–16
7. Cárdenas, C., Liberona, L. J., Molgó, J., Colasante, C., Mignery, G. A., and Jaimovich, E. (2005) *J. Cell Sci.* **118,** 3131–3140
8. Powell, J. A., Carrasco, M. A., Adams, D. S., Drouet, B., Rios, J., Muller, M., Estrada, M., and Jaimovich, E. (2001) *J. Cell Sci.* **114,** 3673–3683
9. Carrasco, M. A., Riveros, N., Rios, J., Muller, M., Torres, F., Pineda, J., Lantadilla, S., and Jaimovich, E. (2003) *Am. J. Physiol.* **284,** C1438–C1447
10. Cárdenas, C., Muller, M., Jaimovich, E., Perez, F., Buchuk, D., Quest, A. F., and Carrasco, M. A. (2004) *J. Biol. Chem.* **279,** 39122–39131
11. Powell, J. A., Molgó, J., Adams, D. S., Colasante, C., Williams, A., Bohlen, M., and Jaimovich, E. (2003) *J. Neurosci.* **23,** 8185–8192
12. Rebecchi, M. J., and Pentyala, S. N. (2000) *Physiol. Rev.* **80,** 1291–1335
13. Rhee, S. G., (2001) *Annu. Rev. Biochem.* **70,** 281–312
14. Eltit, J. M., Hidalgo, J., Liberona, J. L., and Jaimovich, E. (2004) *Biophys. J.* **86,** 3042–3051
15. Várnai, P., Rother, K. I., and Balla, T. (1999) *J. Biol. Chem.* **274,** 10983–10989
16. Stoyanova, S., Bulgarelli-Leva, G., Kirsch, C., Hanck, T., Klinger, R., Wetzker, R., and Wymann, M. P. (1997) *Biochem. J.* **324,** 489–495
17. Bondeva, T., Pirola, L., Bulgarelli-Leva, G., Rubio, I., Wetzker, R., and Wymann, M. P. (1998) *Science* **282,** 293–296
18. Rameh, L. E., Arvidsson, A., Carraway, K. L., 3rd, Couvillon, A. D., Rathbun, G., Crompton, A., VanRenterghem, B., Czech, M. P., Ravichandran, K. S., Burakoff, S. J., Wang, D. S., Chen, C. S., and Cantley, L. C. (1997) *J. Biol. Chem.* **272,** 22059–22066
19. Koch, W. J., Inglese, J., Stone, W. C., and Lefkowitz, R. J. (1993) *J. Biol. Chem.* **268,** 8256–8260
20. Traynor-Kaplan, A. E., Thompson, B. L., Harris, A. L., Taylor, P., Omann, G. M., and Sklar, L. A. (1989) *J. Biol. Chem.* **264,** 15668–15673
21. Shah, A. S., White, D. C., Emani, S., Kypson, A. P., Lilly, R. E., Wilson, K., Glower, D. D., Lefkowitz, R. J., and Koch, W. J. (2001) *Circulation* **103,** 1311–1316
22. Koch, W. J., Hawes, B. E., Inglese, J., Luttrell, L. M., and Lefkowitz, R. J. (1994) *J. Biol. Chem.* **269,** 6193–6197
23. Hamm, H. E. (1998) *J. Biol. Chem.* **273,** 669–672
24. Nakai, J., Sekiguchi, N., Rando, T. A., Allen, P. D., and Beam, K. G. (1998) *J. Biol. Chem.* **273,** 13403–13406
25. Dirksen, R. T., and Beam, K. G. (1999) *J. Gen. Physiol.* **114,** 393–403
26. Lerche, H., Fahlke, C., Iaizzo, P. A., and Lehmann-Horn, F. (1995) *Pflugers Arch.* **429,** 738–747
27. Hartzell, C., Putzier, I., and Arreola, J. (2005) *Annu. Rev. Physiol.* **67,** 719–758
28. Cohen-Armon, M., and Sokolovsky, M. (1993) *J. Biol. Chem.* **268,** 9824–9838
29. Anis, Y., Nurnberg, B., Visochek, L., Reiss, N., Naor, Z., and Cohen-Armon, M. (1999) *J. Biol. Chem.* **274,** 7431–7440
30. Herlitze, S., Hockerman, G. H., Scheuer, T., and Catterall, W. A. (1997) *Proc. Natl. Acad. Sci. U. S. A.* **94,** 1512–1516
31. Catterall, W. A. (2000) *Annu. Rev. Cell Dev. Biol.* **16,** 521–555
32. Bell, D. C., Butcher, A. J., Berrow, N. S., Page, K. M., Brust, P. F., Nesterova, A., Stauderman, K. A., Seabrook, G. R., Nurnberg, B., and Dolphin, A. C. (2001) *J. Neurophysiol.* **85,** 816–827
33. Toutant, M., Gabrion, J., Vandaele, S., Peraldi-Roux, S., Barhanin, J., Bockaert, J., and Rouot, B. (1990) *EMBO J.* **9,** 363–369
34. Carrasco, M. A., Sierralta, J., and de Mazancourt, P. (1994) *Arch. Biochem. Biophys.* **310,** 76–81
35. Smrcka A. V., and Sternweis, P. C. (1993) *J. Biol. Chem.* **268,** 9667–9674
36. Wang, T., Dowal, L., El-Maghrabi, M. R., Rebecchi, M., and Scarlata, S. (2000) *J. Biol. Chem.* **275,** 7466–7469
37. Stoyanov, B., Volinia, S., Hanck, T., Rubio, I., Loubtchenkov, M., Malek, D., Stoyanova, S., Vanhaesebroeck, B., Dhand, R., Nurnberg, B., Gierschik, P., Seedorf, K., Hsuan, J. J., Waterfield, M. D., and Wetzker, R. (1995) *Science* **269,** 690–693
38. Brock, C., Schaefer, M., Reusch, H. P., Czupalla, C., Michalke, M., Spicher, K., Schultz, G., and Nurnberg, B. (2003) *J. Cell Biol.* **160,** 89–99
39. Hirsch, E., Katanaev, V. L., Garlanda, C., Azzolino, O., Pirola, L., Silengo, L., Sozzani, S., Mantovani, A., Altruda, F., and Wymann, M. P. (2000) *Science* **287,** 1049–1053
40. Wymann, M. P., Zvelebil, M., and Laffargue, M. (2003) *Trends. Pharmacol. Sci.* **24,** 366–376
41. Patrucco, E., Notte, A., Barberis, L., Selvetella, G., Maffei, A., Brancaccio, M., Marengo, S., Russo, G., Azzolino, O., Rybalkin, S. D., Silengo, L., Altruda, F., Wetzker, R., Wymann, M. P., Lembo, G., and Hirsch, E. (2004) *Cell* **118,** 375–387
42. Quignard, J. F., Mironneau, J., Carricaburu, V., Fournier, B., Babich, A., Nurnberg, B., Mironneau, C., and Macrez, N. (2001) *J. Biol. Chem.* **276,** 32545–32551
43. Vecchione, C., Patrucco, E., Marino, G., Barberis, L., Poulet, R., Aretini, A., Maffei, A., Gentile, M. T., Storto, M., Azzolino, O., Brancaccio, M., Colussi, G. L., Bettarini, U., Altruda, F., Silengo, L., Tarone, G., Wymann, M. P., Hirsch, E., and Lembo, G. (2005) *J. Exp. Med.* **201,** 1217–1228
44. Viard, P., Exner, T., Maier, U., Mironneau, J., Nurnberg, B., and Macrez, N. (1999) *FASEB J.* **13,** 685–694
45. Le Blanc, C., Mironneau, C., Barbot, C., Henaff, M., Bondeva, T., Wetzker, R., and Macrez, N. (2004) *Circ. Res.* **95,** 300–307
46. Fosset, M., Jaimovich, E., Delpont, E., and Lazdunski, M. (1983) *J. Biol. Chem.* **258,** 6086–6092
47. Milting, H., Heilmeyer, L. M., Jr., and Thielecze, R. (1994) *FEBS Lett.* **345,** 211–218